Radiobiological and physical effects of patient setup errors during whole breast irradiation

S.R. Lee, M.J. Kim, S.H. Park, M.Y. Lee, T.S. Suh*

Department of Biomedical Engineering, College of Medicine, The Catholic University of Korea, Seoul, Korea

► *Original article*

Corresponding authors:
Dr. Tae-Suk Suh,
Fax: + 82 2 2258 7232
E-mail:
suhsanta@catholic.ac.kr

ABSTRACT

Background: The dose-related effects of patient setup errors on bio-physical indices were evaluated for the conventional wedge (CW) and field-in-field (FIF) whole breast irradiation techniques (WBI). ***Materials and Methods:*** The treatment plans of 10 patients receiving left WBI were retrospectively selected for evaluation. The bio-physical effects of dose variations were evaluated by shifting the isocenters and gantry-angles of the treatment plans. Dose-volume histograms of the planning target volume (PTV), heart, and lungs were generated, and the conformity index (CI), homogeneity index (HI), tumor control probability (TCP), and normal tissue complication probability (NTCP) were determined. ***Results:*** The D95 of the PTV for an "isocenter shift plan" with a posterior direction decreased by approximately 15%, and the TCP of the PTV decreased by approximately 50% for the FIF technique and by 40% for the CW; however, the NTCPs of the lungs and heart increased for both techniques. Increasing the gantry-angle decreased the TCPs of the PTV by 24.4% (CW) and by 34% (FIF). The NTCPs of the lungs and heart for the two techniques differed by only 3%. The CIs and HIs for the CW case were higher than the corresponding values obtained for the FIF case. Significant differences were observed between the two techniques (p<0.01). ***Conclusion:*** Our results revealed that the biophysical properties of the FIF case were more sensitive to setup errors than those in the CW case. The radiobiological-based analysis could be detected significant dosimetric errors and provided a practical patient quality assurance method for guiding the bio-physical effects.

Keywords: *Setup error, field-in-field, whole breast irradiation, biological indices.*

INTRODUCTION

A combination of breast-conserving therapy and post-operative whole breast radiotherapy has become a widely accepted and routine treatment for early-stage breast cancer [1-3]. In conventional radiotherapy, the delivery of doses exceeding the prescribed dose can have physical aftereffects, such as the formation of hot spots [9]. Radiation-induced toxicity can cause non-breast cancer-related death, mainly due to cardiac or pulmonary disease [5, 6]. Fibrosis, in particular, is a significant side effect of breast radiotherapy. Several studies have used NTCP modeling methods to predict post-radiotherapy fibrosis and quantify the expected side effects, such as fibrosis, cardiovascular disease, and lung cancer [7, 8].

The delivery of a planned dose distribution during breast radiotherapy may be altered by several factors, including patient shifting movements, patient rotational movements, breast shifting, and breast rotation [10]. Previous studies have estimated the magnitude of setup errors by simulating situations in which the isocenter and gantry angle in the radiation treatment planning system were shifted [11-14]. The dosimetric impact of setup errors was reported by Prabhakar *et al.* [11] who concluded that setup errors in the isocenter based on

physical indices should be kept strictly below 0.3 cm. Furuya *et al.* [12] investigated the impacts of breast motion and setup errors by shifting the isocenter. They found that the dosimetric impact of anterior–posterior breathing motions on the physical characteristics was largest during whole-breast irradiation procedures.

As summarized above, previous studies have investigated the effects of setup errors on physical indices without considering biological effects. This study evaluated the radiobiological and physical results of patient setup errors using inverse verification as a quality assurance (QA) method and suggested the use of a dose painting method to estimate biological parameters, such as the NTCP and tumor control probability (TCP) as a measure of clinically significant errors. This study was conducted using conventional wedge (CW) and field-in-field (FIF) whole breast irradiation techniques.

MATERIALS AND METHODS

Whole breast irradiation planning under a variety of scenarios
Patient selection

The retrospective study described here examined the medical records of 10 patients with early-stage left breast cancer who received whole breast irradiation at Uijeongbu St. Mary's hospital. The Institutional Review Board approved the study (UC14RISI0127). All patients underwent free breathing CT while lying supine with their ipsilateral arm raised above their head. Slice images were acquired at a thickness of 2.5 mm.

Dosimetry planning

All treatment were generated using the Eclipse treatment planning system (Varian Associates, Palo Alto, CA). Treatment planning for whole breast irradiation was performed using two tangential fields and one of two techniques (CW and FIF). The prescription dose used in our study was 50.4 Gy, administered in 28 fractions. Conventional radiotherapy involves application of 45–50 Gy to the whole breast in

wedged tangential fields [4]. All contouring in this study was performed in accordance with the Radiation Therapy Oncology Group 0413 guidelines [15]. Organs at risk (OARs) (the ipsilateral breast, ipsilateral lungs, and heart) were contoured for evaluation, and the breast clinical target volume (CTV) included a 97% isodose line of the prescription dose excluding the 5 mm below the skin surface. Although our study focused on the planning target volume (PTV), the results are applicable to the CTV because the PTV and CTV are generally in good agreement. The photon beam energy was 6 MV, and the treatment plan was calculated by applying an anisotropic analytical algorithm (version 10.0.28) included inhomogeneity correction because the breast treatment fields included a considerable portion of the lungs [28, 29].

The "original plan" for each patient was created using the general clinical planning methods described above. The most important process in our study was the generation of an "isocenter shift plan (IS plan)" and a "gantry angle shift plan (GS plan)" for evaluating the dose distribution as variation of the isocenter position and gantry angle, respectively. The total number of treatment plans was 360 (36 treatment plans per patient). The isocenter for each plan was shifted 0.5 cm to the right–left (RL), along the superior–inferior (SI), or along the anterior–posterior (AP) respectively as described by Kinoshita *et al.* [14]. Some studies suggest that gantry angle variations of up to 8° can provide to dosimetric errors [17, 18]. We assumed that setup errors slightly altered the breast shape. To compensate this effect, we inversely moved the gantry angle to simulate setup errors. The gantry angle was shifted 2.5°–10° clockwise or counterclockwise at intervals of 2.5° in each tangential field. The delivery conditions of the original plan, except for the adjustments to the isocenter and gantry angle, were used in the IS plans and GS plans.

Plan evaluation and analysis
Physical evaluation

The performances of the planning techniques were analyzed by analyzing the dose–volume

Int. J. Radiat. Res., Vol. 15 No. 4, October 2017

344

histograms (DVHs), the mean dose of the PTV, the minimum dose needed to cover 95% of the volume of the PTV (D_{95}), the relative volume of the PTV that received at least 95% of the prescribed dose (V_{95}), and the volumes that received greater than 20 Gy in the ipsilateral lungs and 40 Gy in the heart.

Physical evaluations were conducted using the conformity index (CI) and the heterogeneity index (HI) [16]. The CI evaluated the appositeness of the PTV for the prescription isodose volume in the treatment plans. The HI estimates the homogeneity of the PTV. The CI and HI calculations are presented below [eq. (1)].

$$CI = \frac{V_{PTV} \times V_{TV}}{TV^2_{PV}} \qquad (1)$$

Where, V_{PTV} is the volume of the PTV, V_{TV} is the treatment volume of the prescribed isodose lines, and TV_{PV} is the volume of the V_{PTV} within the V_{TV} [eq. (2)]. Smaller CIs indicated better conformity.

$$HI = \frac{D_{5\%}}{D_{95\%}} \qquad (2)$$

Where, $D_{5\%}$ and $D_{95\%}$ are the minimum doses delivered to 5 and 95% of the PTV, respectively. Smaller HIs indicate better homogeneity.

Radiobiological evaluation

The radiobiological effects were evaluated by calculating the standard effective dose (SEDi) [eq. (3)], TCP [eq. (4)], and NTCP [eq. (5)] using the parameters listed in Table 1 and 2. We performed our analysis using the phenomenological TCP and NTCP model because of its computational simplicity for acquiring voxel-based iso-TCP and NTCP maps [20, 31, 32].

$$SED_i = nd_i \left(1 + \frac{d_i}{(\alpha/\beta)}\right) \Big/ \left(1 + \frac{d_f}{(\alpha/\beta)}\right) \qquad (3)$$

$$TCP(\{D\}) = \prod_{i=1}^{R}[TCP_i(\{SED_i\})]^{v_i}$$

$$= \prod_{i=1}^{R}\left[\frac{1}{1+\left(\frac{TCD_{50}}{SED_i}\right)^{4\gamma_{50}}}\right]^{v_i} , \qquad \sum_{i=1}^{R}v_i = 1 \qquad (4)$$

$$NTCP(\{D\}) = \prod_{i=1}^{R}[NTCP_i(\{SED_i\})]^{v_i}$$

$$= 1 - \prod_{i=1}^{R}\left[1 - \frac{1}{1+\left(\frac{TD(v_{eff})^i_{50}}{SED_i}\right)^{4\gamma_{50}}}\right]^{v_i} , \qquad \sum_{i=1}^{R}v_i = 1 \qquad (5)$$

The values of the TCD_{50}, TD_{50}, and γ_{50} were determined from clinical data (table 1). TCD_{50} is the dose required to achieve 50% TCP. $TD(v_{eff})_{50}$ is the tolerance dose (TD) to the v_{eff} of the organ that produces a complication probability of 50%. γ_{50} is the normalized gradient of the tumor response curve at 50%. The parameters in these equations that were subjected to variations are listed in Table 2. The above methods were performed using the open-source tool CERR [23] and an in-house code based on MATLAB (v.R2010a, Mathworks, Natick, MA).

Statistical analysis

Data from all patients were included in the statistical calculations. The dose indices delivered for each radiotherapy technique were compared and the effects of the setup errors were evaluated by applying the Mann–Whitney test and the Kruskal–Wallis test. A p value of less than 0.05 was considered statistically significant.

Table 1. Radiobiological parameters used to calculate the tumor control probability (TCP) and normal tissue complication probability (NTCP).

Structures		a	γ50	TCD$_{50}$	TD$_{50}$	α/β	References
Tumor	Breast	−7.2	2	45.75		10	Willner *et al.* (24)
							Guerrero *et al.* (25)
							Hall *et al.* (26)
Organs -at-risk (OAR)	Heart	3	3		50	1.8−2	Emami *et al.* (27)
	Lung	1	2		24.5	1.8−2	

Table 2. Variables and their definitions.

Symbols	Definition	Equations
n	The fraction number	(3)
d_i	Fractional dose on i-th each voxel	
d_f	Reference dose per fraction	
α/β	The usual ratio of the linear-quadratic model parameters	
R	Total number of subvolumes	(5) ,(4)
v_i	Fractional volume of i-th voxel	

RESULTS

Physical analysis

All physical results are reported as the average of the results obtained from the 10 patients examined here. Figure 1a shows the minimum doses that covered 95% of the volume of the PTV, determined from the physical results obtained from the IS plan. The difference between the delivered doese for the original isocenter and the isocenter shifted along the AP direction was large, as reported previously, because the AP direction was affected by breathing [12, 14]. This difference was statistically significant (p<0.001). As shown in figures 1(b) and 1(c), the physical perspectives of the normal organs changed along with the isocenter shift. The trend was similar to that observed for the PTV, especially along the AP direction. The PTV coverage improved for the "IS plan" executed along the anterior direction; however, the doses delivered to the lungs and heart increased by factors of 1.6 and 3.8, respectively (figure 3a). The D_{95} of the PTV generated by the "IS plan" executed along the posterior direction decreased by approximately 15% in the FIF-based plans, despite the delivery of lower doses to normal organs (figure 1). The physical results obtained from the CW and FIF techniques with isocenter shifts followed similar trends.

The gantry angle shifts in two directions resulted in a decrease in D_{95}, regardless of the angle direction or treatment technique (figure 2). The results obtained from the CW and FIF techniques were similar, and the gradients of the graphs in the counterclockwise direction, generated using either technique, exceeded the gradient obtained in the clockwise direction. The average values obtained from the two techniques differed significantly (p<0.02). We evaluated the relative volume of the acceptable dose for normal organs based on the gantry angle. The results obtained using the CW and FIF techniques were no significant difference. The delivered dose to normal organs (except for the heart) using the GS plan increased in any direction (table 3). For heart cases, the maximum difference was about 48% between origin plan and -10 degree shift plan in both techniques.

The results calculated for the 360 cases revealed that the CIs and HIs obtained using the CW technique were much higher than the values obtained using the FIF technique. This difference was significant (p<0.01). Notably, a shift in the gantry angle and isocenter reduced the homogeneity and conformity of the PTV and increased the magnitude of the errors. A gantry angle shift counterclockwise produced the worst results: the CI was 24.48% of the value obtained using the original plan.

Radiobiological analysis

The biological effects of the isocenter shifts (particularly those obtained using the FIF technique) were evaluated by mapping the DVHs and NTCP/TCP values onto the CT images (figure 3). The effects of the shifts depended on the shift direction. The IS plan with a posterior direction delivered lower doses to the PTV compared to the original plan, and the TCP decreased (table 4). Lower doses were delivered to the OARs (figure 3(a)), and the NTCP declined by approximately 44%. The opposite results were obtained from the IS plan with a superior direction (the NTCP in the normal organs increased and the TCP in the tumor decreased).

Figures 4 and 5 show the DVHs and radiobiological maps of the CT images obtained using the CW technique. The gantry angle was shifted clockwise and counterclockwise, respectively. The shift direction did not significantly affect the DVHs or NTCPs of the normal organs. As the gantry angle shifted toward the maximum degree of displacement,

Int. J. Radiat. Res., Vol. 15 No. 4, October 2017

346

the NTCPs of the original and shifted (either direction) plans differed by less than 1%, regardless of the technique applied (table 4). By contrast, the TCPs and doses delivered to the PTV were lower in the shifted plans than in the original plans. The TCP and NTCP maps on the CT images revealed the positions that received low doses and the differences between the

radiobiological effects due to shifts in the angle direction. The radiation fields were not applied to the upper or lower parts of the PTV as the gantry angle was shifted along the clockwise or counterclockwise direction, respectively (figures 4b and 5b). For this reason, the voxel-based NTCP/TCP method was recommendable in our study.
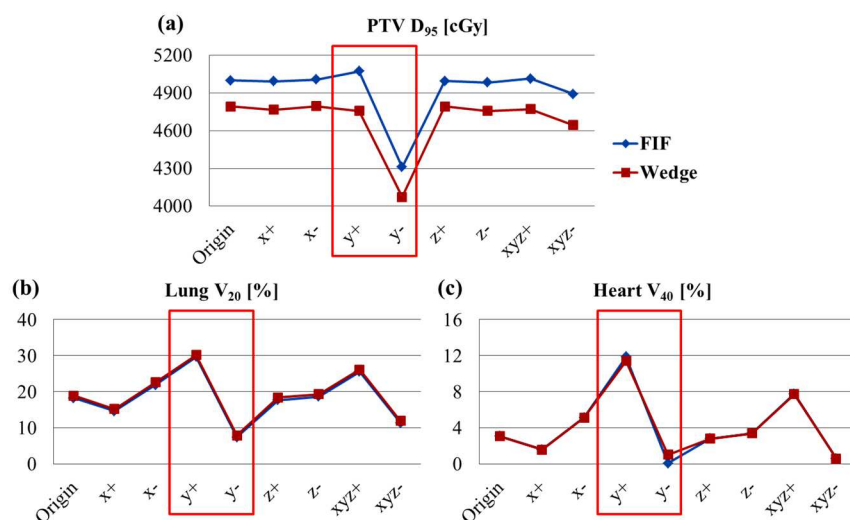

Figure 1. The physical results of the isocenter shifts are shown for (a) a minimum dose that covers 95% of the planning tumor volume (PTV), (b) relative volumes receiving an excess of 20 Gy in the ipsilateral lungs, and (c) relative volumes receiving an excess of 40 Gy in the heart.
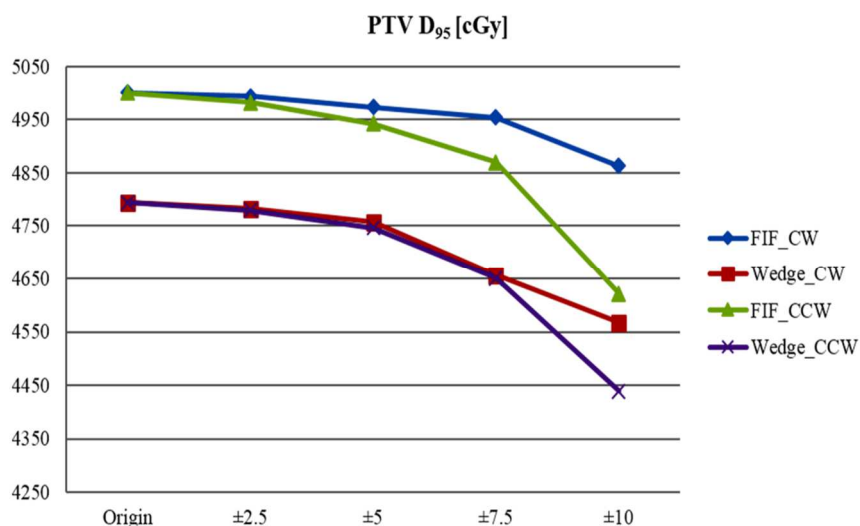

Figure 2. The physical results of bi-directional gantry angle shifts for a minimum dose that covers 95% of the planning tumor volume (PTV) in two directions for the conventional wedge technique and field-in-field technique.
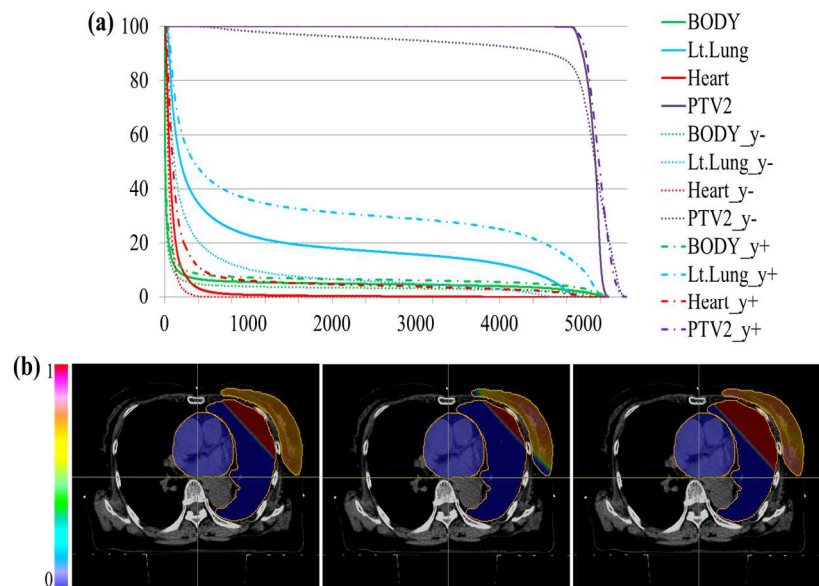
347

Int. J. Radiat. Res., Vol. 15 No. 4, October 2017

Figure 3. The physical and radiobiological results of isocenter shifts for a breast cancer patient. (a) Dose volume histogram (DVH), (b) tumor control probability (TCP) and normal tissue complication probability (NTCP) mapping onto computed tomography (CT) images of the principal structures. The field-in-field technique was used. The origin, negative y direction, and positive y direction are shown in order.

Table 3. Effects of gantry angle shifts on normal tissue for conventional wedge and field-in-field techniques.

			Origin	Gantry angle shift							
				Clockwise				Conter-clockwise			
				+°2.5	+°5	+°7.5	+°10	−°2.5	−°5	-°7.5	-°10
Field-in-field technique	Heart V40 [%]	Mean	2.761	2.413	2.134	1.919	1.739	3.209	3.770	4.467	5.325
		SD*	2.289	2.104	1.959	1.844	1.752	2.535	2.851	3.244	3.705
	Lung V20 [%]	Mean	17.391	17.455	17.586	17.789	18.058	17.380	17.414	17.471	17.532
		SD	3.704	3.691	3.712	3.773	3.899	3.751	3.821	3.913	3.996
Conventional wedge technique	Heart V40 [%]	Mean	2.793	2.439	2.156	1.940	1.765	3.263	3.812	4.511	5.375
		SD	2.313	2.130	1.986	1.874	1.781	2.565	2.868	3.256	3.707
	Lung V20 [%]	Mean	18.320	18.411	18.569	18.844	19.159	18.278	18.285	18.311	18.336
		SD	3.816	3.817	3.845	3.955	4.083	3.861	3.927	4.0181	4.100

Table 4. Tumor control probabilities (TCPs) and normal tissue complication probabilities (NTCPs) in various situations for conventional wedge and field-in-field techniques.

			Origin	Gantry angle shift				Isocenter shift			
				+°5	+°10	−°5	−°10	+y	−y	+xyz	−xyz
Field-in-field technique	PTV	TCP [%]	87.190	79.590	71.200	68.550	53.150	73.330	39.230	68.390	66.960
	Lung	NTCP [%]	10.636	12.481	12.553	13.005	13.51	23.778	7.4304	18.01	9.1419
	Heart		5.2214	5.1461	5.1064	5.3464	5.5614	6.4395	4.905	5.731	5.0068
Conventional wedge technique	PTV	TCP [%]	78.910	67.660	60.060	66.580	54.470	69.700	38.680	68.540	64.270
	Lung	NTCP [%]	12.401	14.271	14.376	14.788	15.374	25.917	8.5199	20.421	10.516
	Heart		5.8527	5.7517	5.6929	6.0137	6.2783	7.2404	5.4656	6.4574	5.612

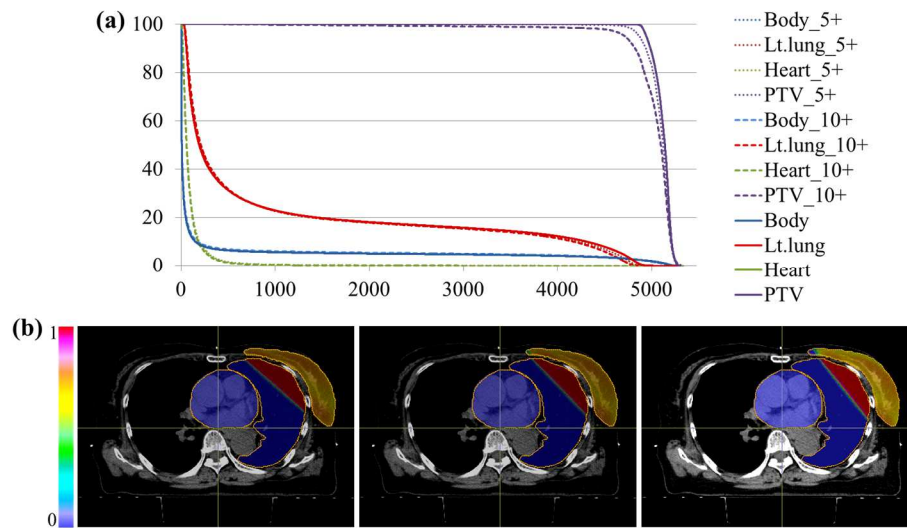*Int. J. Radiat. Res., Vol. 15 No. 4, October 2017*

348

Figure 4. The physical and radiobiological results of clockwise gantry angle shifts for a breast cancer patient. (a) Dose volume histogram (DVH), (b) tumor control probability (TCP) and normal tissue complication probability (NTCP) mapping of computed tomography (CT) images of the principal structures. The conventional wedge technique was used. The origin, a 5-degree shift, and a 10-degree shift are shown in order.
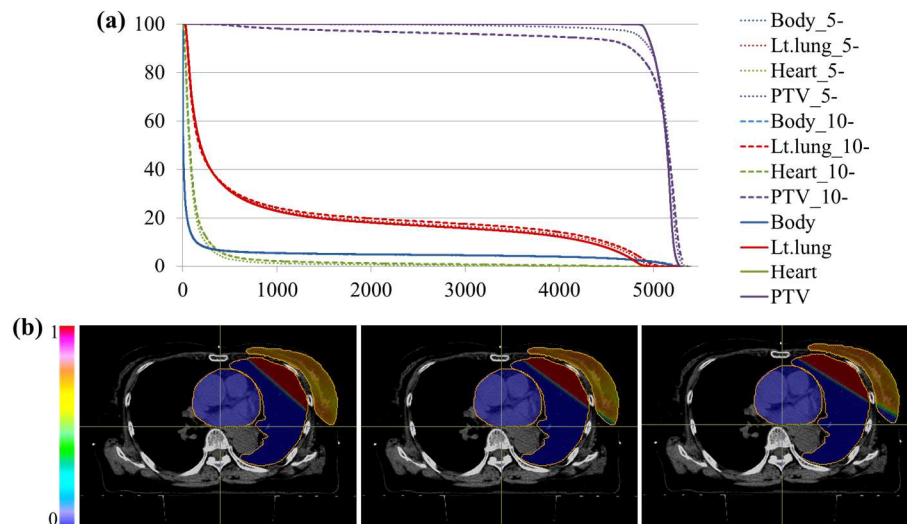

Figure 5. The physical and radiobiological results of counterclockwise gantry angle shifts for a breast cancer patient. (a) Dose volume histogram (DVH), (b) tumor control probability (TCP) and normal tissue complication probability (NTCP) mapping onto computed tomography (CT) images of the principal structures. The conventional wedge technique was used. The origin, a 5-degree shift, and a 10-degree shift are shown in order.

DISCUSSION

Radiation treatment for breast cancer is generally performed 5 days a week. The breast position on each day cannot be assumed to remain constant due to breast tissue flexibility and breathing motions. Errors in positioning the patients' breasts have been quantitatively evaluated in many studies; however, only physical results have been reported [33-37]. The present study examined both the physical and radiobiological effects of positioning errors during breast radiation treatment. The isocenter and gantry angle in the original plan implemented using the CW or FIF techniques were shifted to simulate the patient positioning errors. Left breast radiotherapy typically requires more sensitive radiation treatment planning than right breast radiotherapy because the left breast is close to the heart, and

349

substantial radiation effects on the heart are possible [38-40]. Therefore, the left breast cases were selected to evaluate the side effects on OARs during whole breast irradiation.

The physical results were examined by calculating physical indices, such as the D_{95}, mean dose, and V_{95} of the PTV. Only the value of D_{95} for the PTV is reported because the other parameters followed trends similar to D_{95}. Smaller CIs and HIs indicated better conformity and homogeneity, respectively, in the PTV [41, 42, 43]. In agreement with previous studies [41, 42, 43], the CIs and HIs were significantly smaller for the FIF-based plans than for the CW-based plans, in all cases.

The radiobiological results, particularly the NTCPs, were similar in several simulations, possibly due to the properties of the NTCP curves. Many NTCP curves with different endpoints were used. Rancati *et al.*'s results [30] was illustrated in a graph of an NTCP, revealing that the TD required to reach 50% of the NTCP was 16.1 Gy (saturation was reached at 0–10 Gy) for an endpoint of pneumonitis detection in the CT images. The TD was 25.4 Gy in our study because the endpoint was genesis inflammation of the lung from radiotherapy. This assumption led to smoother NTCP curves than those obtained by Rancati *et al.* [30]. The maximum difference in the mean doses delivered to the lungs in the original plans and the gantry angle shift plans were 1.52 Gy (FIF) and 0.78 Gy (CW). These results suggested that the NTCPs did not differ significantly, thereby explaining the smooth NTCP curves. However, the IS plan revealed that the mean dose to the lungs increased to 16.66 Gy (CW) and 16.23 Gy (FIF). In this instance, the NTCPs were significant (table 4).

Biological results have been recently calculated using radiation treatment planning systems or dosimetry software. These methods are limited in their ability to fully capture biological effects because they only suggest the value of biological results without considering spatial information. It would be difficult to predict the magnitude of NTCP variations, except in a case in which the mean dose to the lung were increased significantly. Sensitive error

detection using biological indices may be obtained using the iso-TCP-NTCP maps generated in the present study. Such maps could provide spatial information that is lacking in the DVHs, which only assess the uniformity of the dose distribution [19]. The biological effects of radiation treatment may be visualized using voxel-based TCP and NTCP methods, as has been demonstrated in prostate cases [20-22]. Intensity-modulated radiation treatment (IMRT) for prostate cancer requires consideration of biological effects because the radiation dose is highly modulated. On the other hand, breast cancer requires evaluation of the biological effects of PTV and OARs because the FIF technique, which is a forward IMRT technique, is widely used along with CW, and breast cancer also many relevant OARs, such as the heart or lung.

In this study, the FIF technique was more sensitive to setup errors than the CW technique; however, dosimetric differences in the setup errors obtained from the FIF technique were relatively small. The physical effects of dose inhomogeneities created during the CW technique due to setup errors were lower than those created during the FIF technique [12]. Despite these results, the FIF technique is more commonly used because dose homogeneity obtained using IMRT cause lower chronic and acute toxicities compared with the dose homogeneities obtained using CW [9].

Although our study was limited to the effects of physical errors that resulted in dose discrepancies, we demonstrated that biological evaluations provided information that was missing from the physical evaluations. Many studies of radiobiological indices have accompanied the growing interest in biology-based QA in radiotherapy [20, 44]. Biological indices have two limitations: (1) they are phenomenological rather than predictive, and (2) model parameters are unreliable due to insufficient clinical data [45, 46]. Medical physicists must carefully select assessment indices to appropriately evaluate the biological effects on clinical cases, given study endpoints and the overall study goals. This study suggested that a biological evaluation, in addition to a physical

Int. J. Radiat. Res., Vol. 15 No. 4, October 2017

350

evaluation conducted using our QA method, should improve QA accuracy for validating setup errors in the FIF technique.

CONCLUSION

Biological indices obtained using the iso-TCP and NTCP maps were sensitive to errors not present in the physical indices. The iso-TCP and NTCP maps provided a useful and practical method for evaluating critical biophysical effects. Our finding demonstrated that physical and biological indices measured in simulations can detect a variety of errors that arise in breast radiotherapy applied using either the CW or FIF technique.

ACKNOWLEDGEMENTS

***Conflicts of interest**: Declared none.*

REFERENCES

1. Early Breast Cancer Trialists's Collaborative Group (EBCTCG) (2011) Effect of radiotherapy after breast-conserving surgery on 10-year recurrence and 15-year breast cancer death: meta-analysis of individual patient data for 10 801 women in 17 randomized trials. *Lancet, 378: 1707-16.*

2. Veronesi U, Luini A, Vecchio MD, Greco M, Galimberti V, Merson M, *et al*. (1993) Radiotherapy after breast-preserving surgery in women with localized cancer of the breast. *N Engl J Med, 328: 1587-91*.

3. Vincent VH and Verschraegen C (2004) Breast-conserving surgery with or without radiotherapy: pooled-analysis for risks of ipsilateral breast tumor recurrence and mortality. *J Natl Cancer Inst, 96: 115-21*.

4. Kutcher GJ, Smith AR, Fowble BL, Owen JB, Hanlon A, Wallace M, *et al*. (1996) Treatment planning for primary breast cancer: a patterns of care study. *Int J Radiat Oncol Biol Phys, 36: 731-37*.

5. Hurkmans CW, Borger JH, Bos LJ, Horst A, Pieters BR, Lebesque JV, *et al*. (2000) Cardiac and lung complication probabilities after breast cancer irradiation. *Radiother Oncol, 55: 154-51*.

6. Mcgale P, Darby SC, Hall P, Adolfsson J, Bengtsson N-O, Bennet AM, *et al*. (2011) Incidence of heart disease in 35,000 women treated with radiotherapy for breast cancer in Denmark and Sweden. *Radiother Oncol, 100: 167-75*.

7. Patel RR, Becker SJ, Das RK, Mackie TR (2007) A dosimetric comparison of accelerated partial breast irradiation techniques: multicatheter interstitial brachytherapy, tree-dimensional conformal radiotherapy, and supine versus prone helical tomotherapy. *Int J Radiat Oncol Biol Phys, 68: 935-42*.

8. Basu KSJ, Bahl A, Subramani V, Sharma DN, Rath GK, Julka PK (2008) Normal tissue complication probability of fibrosis in radiotherapy of breast cancer: accelerated partial breast irradiation vs conventional external-beam radiotherapy. *J Cancer Res Ther, 4: 126-30*.

9. Harsolia A, Kestin L, Grills I, Wallace M, Jolly S, Jones C, *et al*. (2007) Intensity-modulated radiotherapy results in significant decrease in clinical toxicities compared with conventional wedge-based breast radiotherapy. *Int J Radiat Oncol Biol Phys, 68: 1375-80*.

10. Mouric AV, Kranen SV, Hollander SD, Sonke JJ, Herk M, Vroegindeweij CVV (2011) Effects of setup errors and shape changes on breast radiotherapy. *Int J Radiat Oncol Biol Phys, 79: 1557-64*.

11. Prabhakar R, Rath GK, Julka PK, Ganesh T, Haresh KP, Rakesh C, *et al*. (2007) Simulation of dose to surrounding normal structures in tangential breast radiotherapy due to setup errors. *Med Dosim, 33: 81-85*.

12. Furuya T, Sugimoto S, Kurokawa C, Ozawa S, Karasawa K, Sasai K (2013) The dosimetric impact of respiratory breast movement and daily setup error on tangential whole breast irradiation using conventional wedge, field-in-field and irregular surface compensator techniques. *J Radiat Res, 54: 157-65*.

13. Baglan KL, Sharpe MB, Jaffray D, Frazier RC, Fayad J, Kestin LL, *et al*. (2003) Accelerated partial breast irradiation using 3D conformal radiation therapy (3D-CRT). *Int J Radiat Oncol Biol Phys, 55: 302-11*.

14. Kinoshita R, Shimizu S, Taguchi H, Katoh N, Fujino M, Onimaru R, *et al*. (2008) Three-dimensional intrafractional motion of breast during tangential breast irradiation monitored with high-sampling frequency using a real-time tumor-tracking radiotherapy system. *Int J Radiat Oncol Biol Phys, 70: 931-34*.

15. Wolmark N, Curran WJ, Vicini F, White J, Arthur D, Kuske R, *et al*. (2011) NSABP Protocol B39/RTOG Protocol 0413: A randomized phase III study of conventional whole breast irradiation versus partial breast irradiation for women with stage 0, Ⅰ or Ⅱ breast cancer. http://rpc.mdanderson.org/rpc/credentialing/files/B39_Protocol1.pdf (7 March 2011, date last accessed)

16. Lee TF, Ting HM, Chao PJ, Fang FM (2012) Dual arc volumetric-modulated arc radiotherapy (VMAT) of nasopha-

351

Int. J. Radiat. Res., Vol. 15 No. 4, October 2017

ryngeal carcinomas: a simultaneous integrated boost treatment plan comparison with intensity-modulated radiotherapies and single arc VMAT. *Clin Oncol, 24: 196-207*.

17. Guckenberger M, Meyer J, Vordermark D, Baier K, Wilbert J, Flentje M (2006) Magnitude and clinical relevance of translational and rotational patient setup errors: a cone-beam CT study. *Int J Radiat Oncol Biol Phys, 65: 934-42*.

18. Probst H and Griffiths S (2006) Moving to a high-tech approach to the irradiation of early breast cancer: is it possible to balance efficacy, morbidity and resource use? *Clin Oncol, 18: 268-75*.

19. Kim Y and Tome WA (2008) On voxel based iso-tumor-control probability and iso-complication maps for selective boosting and selective avoidance intensity-modulated radiotherapy. *Imaging Decis, 12: 42-50*

20. Park JY, Lee JW, Chung JB, Choi KS, Kim YL, Park BM, Kim Y, *et al.* (2012) Radiobiological model-based bio-anatomical quality assurance in intensity-modulated radiation therapy for prostate cancer. *J Radiat Res, 53: 978-88*.

21. Kim Y and Tome WA (2010) Dose-painting IMRT optimization using biological parameters. *Acta Oncol, 49: 1374-84*.

22. Kim Y and Tome WA (2006) Risk-adaptive optimization: selective boosting of high-risk tumor subvolumes. *Int J Radiat Oncol Biol Phys, 66: 1528-42*.

23. Deasy JO, Blanco AI, Clark VH (2003) CERR: a computational environment for radiotherapy research. *Med Phys, 30: 979-85*.

24. Willner J, Baier K, Caragiani E, Tschammler A, Flentje M (2002) Dose, volume, and tumor control predictions in primary radiotherapy of non-small-cell lung cancer. *Int J Radiat Oncol Biol Phys, 52: 382-89*.

25. Guerrero M and Li XA (2003) Analysis of a large numver of clinical studies for breast cancer radiotherapy: estimation of radiobiological parameters for treatment planning. *Phys Med Biol, 48: 3307-26*.

26. Hall EJ (2000) Radiobiology for the radiologist. 5th ed. Lippincott Williams & Wilkins. USA.

27. Emami B, Lyman J, Brown A, Cola L, Goitein M, Munzenrider JE, *et al.* (1991) Tolerance of normal tissue to therapeutic irradiation. *Int J Radiat Oncol Biol Phys, 21: 109-122*.

28. Breitman K, Rathee S, Newcomb C, Murray B, Robinson D, Field C, *et al.* (2007) Experimental validation of the Eclipse AAA algorithm. *J Appl Clin Med Phys, 8: 76-92*.

29. Ronde HS and Hoffmann L (2009) Validation of Varian's AAA algorithm with focus on lung treatments. *Acta Oncol, 48: 209-15*.

30. Rancati T, Wennberg B, Lind P, Svane G, Gagliardi G (2007) Early clinical and radiological pulmonary complications following breast cancer radiation therapy: NTCP fit with four different models. *Radiother Oncol, 82: 308-16*.

31. Kim Y and Tome W (2008) Optimization of radiotherapy using biological parameters. *Cancer Treat Res, 139: 257-78*.

32. Luxton G, Keall PJ, King CR (2008) A new formula for normal tissue complication probability (NTCP) as a function of equivalent uniform dose (EUD). *Phys Med Bio, 53: 23-36*.

33. Sidhu S, Sidhu NP, Lapointe C, Gryschuk G (2006) The

effects of intrafraction motion on dose homogeneity in a breast phantom with physical wedges, enhanced dynamic wedges, and ssIMRT. *Int J Radiat Oncol Biol Phys, 66: 64-75*.

34. Sharon QX, White J, Rabinovitch R, Merrell K, Sood A, Bauer A, *et al.* (2010) Respiratory Organ Motion and Dosimetric Impact on Breast and Nodal Irradiation. *Int J Radiat Oncol Biol Phys, 78: 609-17*.

35. Liu Q, Mcdermott P, Burmeister J (2007) Effect of respiration motion on the delivery of breast radiotherapy using SMLC intensity modulation. *Med Phys, 34: 347–51*.

36. Chui CS, Yorke E, Hong L (2003) The effects of intrafraction organ motion on the delivery of intensity-modulated field with a multileaf collimator. *Med Phys, 30: 1736–46*.

37. George R, Keall PJ, Kini VR, Vedam SS, Siebers JV, Wu Q, *et al.* (2003) Quantifying the effect of intrafraction motion during breast IMRT planning and dose delivery. *Med Phys, 30: 552–62*.

38. Cho BCJ (2005) Improving radiotherapy treatment for left-sided breast cancer. *Med Phys, 32: 641*.

39. Tsai PF, Lin SM, Lee SH, Yeh CY, Huang YT, Lee CC, *et al.* (2012) The feasibility study of multiple partial volumetric-modulated arcs therapy in early stage left-sided breast cancer patients. *J Appl Clin Med Phys, 13: 3806*.

40. Goddu SM, Chaudhari S, Hunter MM, Pechenaya OL, Pratt D, Mutic S, *et al.* (2009) Helical tomotherapy planning for left-sided breast cancer patients with positive lymph nodes: comparison to conventional multiport breast technique. *Int J Radiat Oncol Biol Phys, 73: 1243-51*.

41. Murthy KK, Shukeili KA, Kumar SS, Davis CA, Chandran RR, Namrata S (2010) Evaluation of dose coverage to target volume and normal tissue sparing in the adjuvant radiotherapy of gastric cancers: 3D-CRT compared with dynamic IMRT. *Biomed Imaging Interv J, 6: e29*.

42. Lee TF, Fang FM, Chao PJ, Su TJ, Wang LK, Leung SW (2008) Dosimetric comparisons of helical tomotherapy and step-and-shoot intensity-modulated radiotherapy in nasopharyngeal carcinoma. *Radiother Oncol, 89: 89-96*.

43. Yavas G, Yavas C, Acar H (2012) Dosimetric comparison of whole breast radiotherapy using field in field and conformal radiotherapy techniques in early stage breast cancer. *Int J Radiat Res, 10: 131-138*.

44. Bentzen SM, Bernier J, Davis JB, Horiot JC, Garavaglia G, Chavaudra J, *et al.* (2000) Clinical impact of dosimetry quality assurance programmes assessed by radiobiological modelling of data from the thermoluminescent dosimetry study of the European Organization for Research and Treatment of Cancer. *Eur J Cancer, 36: 615-20*.

45. Cyril V, Julian D, Roustit R, Biffi K, Lantieri C (2013) Biological effects and equivalent doses in radiotherapy: A software solution. *Reports of Practical Oncology & Radiotherapy, 19: 47-55*.

46. Wang XH, Mohan R, Jackson A, Leibel SA, Fuks Z, Ling CC (1995) Optimization of intensity-modulated 3D conformal treatment plans based on biological indices. *Radiother Oncol, 37: 140-52*.

Int. J. Radiat. Res., Vol. 15 No. 4, October 2017

352